

## Scientific Article

# 3,3'-Diindolylmethane Enhances Tumor Regression After Radiation Through Protecting Normal Cells to Modulate Antitumor Immunity



Lijun Li, MD,<sup>a,1</sup> Renxiang Chen, PhD,<sup>a,1</sup> Yun-Tien Lin, MS,<sup>a</sup> Arslon Humayun,<sup>b</sup> Albert J. Fornace Jr, MD,<sup>a,c</sup> and Heng-Hong Li, PhD, MD<sup>a,c,\*</sup>

<sup>a</sup>Department of Oncology, Georgetown University Medical Center, Washington, DC; <sup>b</sup>Georgetown College, Georgetown University, Washington, DC; and <sup>c</sup>Department of Biochemistry, Molecular and Cellular Biology, Georgetown University Medical Center, Washington, DC

Received 12 April 2020; revised 6 September 2020; accepted 13 October 2020

## Abstract

**Purpose:** Preclinical and clinical data indicate that radiation therapy acts as an immune modifier, having both immune-stimulatory and immunosuppressive effects on the tumor-immune microenvironment (TIME). 3,3'-diindolylmethane (DIM) sensitizes tumor cells to radiation and protects mice from lethal doses of total body irradiation. We hypothesize that protecting nontumoral cells from the adverse effects of radiation treatment (RT) may help to correct immunosuppression resulting from radiation.

**Methods and Materials:** We generated tumor graft models using immune-competent and immune-deficient mouse strains. Narrow-beamed radiation was targeted to tumor sites using shielding. Tumor regression was monitored after DIM and RT versus RT alone. The effects of DIM on the efficacy of RT were assessed using immunohistochemistry staining and gene expression profiling. Complete blood counts, clonogenic cell survival assays, and global gene expression profiling of cultured cells were performed to study DIM's radioprotective effects on normal cells.

**Results:** DIM enhanced tumor regression after RT in immune-competent but not immune-deficient mice. Data indicated that DIM increased intratumoral immune cells after RT, contributing to enhanced immunologic responses such as adhesion and antigen processing. DIM protected normal cells from radiation-induced immediate injuries *in vitro* and *in vivo*. Transcriptomic profiling of cultured cells showed that DIM treatment mildly increased expression of some genes that are normally induced after radiation, such as genes involved in cell cycle arrest and apoptosis.

**Conclusions:** In this study, using cultured cells and preclinical breast cancer models, we show that DIM protects normal cells from radiation-induced immediate cellular injury and combination treatment of DIM and radiation potentiates antitumor immune responses and enhances the efficacy of RT.

© 2020 The Authors. Published by Elsevier Inc. on behalf of American Society for Radiation Oncology. This is an open access article under the CC BY-NC-ND license (<http://creativecommons.org/licenses/by-nc-nd/4.0/>).

Sources of support: Research in this publication was supported by NCI of the NIH under award number R01CA184168.

Disclosures: None to report.

Research data are stored in an institutional repository and will be shared upon request to the corresponding author.

\* Corresponding author: Heng-Hong Li, PhD, MD; E-mail: [HL234@georgetown.edu](mailto:HL234@georgetown.edu)

<sup>1</sup> L.L. and R.C. contributed equally to this work.

<https://doi.org/10.1016/j.adro.2020.10.014>

2452-1094/© 2020 The Authors. Published by Elsevier Inc. on behalf of American Society for Radiation Oncology. This is an open access article under the CC BY-NC-ND license (<http://creativecommons.org/licenses/by-nc-nd/4.0/>).

## Introduction

3,3'-diindolylmethane (DIM) is one of the best characterized bioactive compounds found in Cruciferae.<sup>1</sup> The acid-catalyzed dimer of the bioactive indole has long been proposed for use as a cancer prevention agent.<sup>2</sup> DIM has been found to regulate cancer cell proliferation by acting

as an AhR ligand, reducing oxidative stress, activating interferon- $\gamma$ , and modulating estrogen signaling.<sup>1</sup>

Studies also suggest that DIM inhibits radiation therapy and chemotherapy-induced toxicity in normal cells.<sup>3</sup> DIM was found to protect cultured cells against ionizing radiation in clonogenic survival assays by activating ataxia-telangiectasia mutated (ATM) signaling.<sup>4</sup> DIM also protects mice against lethal doses of total body irradiation (TBI) and ameliorates TBI-induced hematopoietic injury by inhibiting oxidative stress responses and hematopoietic cell apoptosis.<sup>5</sup> However, DIM does not protect MDA-MB-231 human breast cancer xenografts in nude mice against fractionated radiation therapy (RT).<sup>4</sup> This preferential protection of normal cells makes DIM an attractive adjuvant to radiation therapy, particularly when high-dose RT results in delayed tissue and organ toxicity.

Recently, the use of RT has been explored to enhance immunotherapy.<sup>6,7</sup> Radiation enhances major histocompatibility complex (MHC) class I expression in tumor cells and increases cytotoxic T lymphocyte recognition of irradiated cells.<sup>8</sup> On the other hand, radiation exhibits immunosuppressive effects on the tumor microenvironment. RT induces expression of the immunosuppressive cytokine TGF- $\beta$ <sup>9,10</sup> and increases infiltration of both regulatory T cells<sup>11</sup> and immunosuppressive myeloid cells.<sup>12</sup> Radiation also leads to higher expression of immune checkpoint ligands, including PD-L1, in tumor cells,<sup>13</sup> as well as PD-1 in T cells.<sup>14</sup>

The importance of tumor immunity warrants an investigation of DIM's effects on the tumor-immune microenvironment (TIME) in response to radiation. In this study, we used a clinically relevant, syngeneic breast cancer model in immunocompetent mice<sup>6</sup> to characterize how DIM influences the TIME and tumor regression after RT.

## Methods and Materials

### Cell cultures and chemical and in vitro treatment

Human breast cancer cell lines MDA-MB-231 and HCC1937 were obtained from the Tissue Culture Shared Resource. Murine breast cancer cell line E0771 and hTERT-immortalized human mammary epithelial cell line (HMEC-hTERT) were kindly provided by our collaborators. HMEC-hTERT cells were cultured in keratinocyte serum-free media (Gibco, Waltham, MA) containing 25 mg/mL of bovine pituitary extract and 5 ng/mL of human recombinant epidermal growth factor. The other cells were cultured in DMEM supplemented with 10% fetal bovine serum. Cells were maintained at 37°C in a 5% CO<sub>2</sub> atmosphere. BR9001, a bioavailability enhancing, self-emulsifying DIM formulation (BioResponse, Boulder, CO) was a kind gift from Dr Michael Zeligs. Subconfluent HMEC-hTERT cells were exposed to

ionizing radiation using a Precision X-RAD 320 irradiator (320 kV, 25 mA) at a dose rate of 0.864 Gy/min. For DIM treatment, the drug was administered 24 hours before irradiation.

### Tumor models and treatments

Immune-competent wild-type C57BL/6J female mice were used as the syngeneic breast tumor model. Athymic nude (CrI:NU(NCr)-*Foxn1*<sup>tm</sup>) and NSG (NOD.Cg-*Prkdc*<sup>scid</sup> *Il2rg*<sup>tm1Wjl</sup>/SzJ) mice were purchased from Charles River and the Jackson Laboratory, respectively, and used as immunodeficient models. Tumor cells were injected subcutaneously in the right dorsal flank. Mice were randomized to 4 groups (n = 5-8): (1) vehicle (SV); (2) DIM (SD); (3) radiation + vehicle (RV); and (4) radiation + DIM (RD). Anesthetized mice were subjected to tumor site targeted radiation using narrow-beamed radiation with a shield (Precision X-Ray Inc, North Branford, CT). DIM was administered intraperitoneally at the concentration of 75 mg/kg. Mice were given 6 Gy per day at 0.864 Gy/min on 4 consecutive days. DIM was administered daily from 1 day before irradiation to 1 day after the last fraction. These experiments have been repeated 3 times using biological replicates. All animal experiments were performed in accordance with the Institutional Animal Care and Use Committee.

### Immunohistochemistry (IHC)

Mice were sacrificed at 12 days after the date when the last radiation fraction was delivered, and tumor tissues were harvested. Harvested tumor tissues were subjected to IHC. For each tumor section, 12 different random fields of view were imaged at 400 $\times$  magnification. Average integrated density for each treatment group (n = 8) was measured using ImageJ software installed with the plugin including color deconvolution function.

### NanoString gene expression analysis

Total RNA was extracted from flash-frozen tumor tissues. Tumor samples from 5 mice in each group were used. RNA quality was assessed using an Agilent 2100 Bioanalyzer (Agilent, Santa Clara, CA). One hundred nanograms of tumor tissue RNA was subjected to gene expression profiling using the nCounter PanCancer Immune Profiling Panel (NanoString Tech, Seattle, WA). Sample labeling, hybridization, and scanning were performed using the nCounter MAX Analysis System. Quality control metrics were reported using the nSolver Analysis Software v4.0. Raw read counts normalization, differential expression, cell type profiling, and pathway score analysis were performed using nCounter Advanced Analysis Software v2.0.

## Microarray and data analysis

Microarray analysis was performed on 3 replicates of each treatment. Detailed methods can be found in the [supplementary materials](#). Identification of differentially expressed genes was performed by filtering the data set using  $P < .05$  and a treatment-to-control ratio greater than 1.7, as well as by 1-way analysis of variance (ANOVA) statistical analysis followed by Benjamin-Hochberg multiple testing. Differential genes that met these statistical criteria in any of the 3 analyses (sham vs 3 Gy, sham vs DIM, and sham + DIM vs 3 Gy + DIM) were identified. In total, there were 1885 genes. These genes were subjected to 2-dimensional clustering visualized using Genesis (genome.tugraz.at) and the Ingenuity Pathway Analysis (Qiagen, Redwood City, CA).

## Statistical analysis

The data are expressed as mean  $\pm$  standard error of the mean (SEM). Significance was analyzed by 2-way ANOVA and 1-way ANOVA. Multiple comparisons were performed using GraphPad Prism 6 Software (GraphPad Software, San Diego, CA). Values were considered significant at  $P < .05$ , except in the NanoString cell type analysis, where the significant cutoff was set at  $P < .1$ .

## Results

### DIM enhances tumor regression after radiation treatment in wild-type but not immunodeficient mice

Mouse models with engrafted tumors were used to test the effect of DIM on the growth and radiosensitivity in

tumors. Wild-type C57BL/6J or immunodeficient mice bearing subcutaneously engrafted breast cancer cells were treated with localized radiation in the absence or presence of DIM treatment. Assessment of growth of E0771 cells in syngeneic C57BL/6J mice (Fig 1A) showed a significant improvement in mice that received combined RD treatment compared with radiation alone (RV). In contrast, growth of E0771 tumors in athymic nude mice showed no significant difference in the efficacy of RT when combined with DIM (Fig 1B). For both models, the SV and SD groups showed no significant difference in tumor growth, suggesting that DIM treatment alone had no influence on tumor growth.

The unexpected difference between wild-type and athymic nude mice that received RD treatment suggests that functional T cells are essential to the efficacy of DIM when combined with RT. Similarly, RT and DIM combination did not enhance efficacy of radiation treatment on xenografts of 2 human breast cancer cell lines, MDA-MB-231 and HCC1937, in another immunodeficient NSG model (Fig E1A and E1B). Mouse body weight was measured and is shown in Figure E2.

### DIM increased intratumoral immune cells after RT

Because DIM showed no independent effect by itself on tumor growth and enhanced the efficacy of RT only in immunocompetent mice, we hypothesized that DIM augments antitumor immunity after radiation. To evaluate changes within discrete cellular populations, immune gene expression profiling of tumors harvested from wild-type C57BL/6J hosts was performed using the nCounter PanCancer Immune Profiling Panel. The quality control plot (Fig E3) indicates the validity of each cell type's measurements. Log-scaled scores of cell types that meet the quality control validity threshold ( $P < .1$ ) are plotted in Figure 2A. Abundance of macrophages, T cells, and

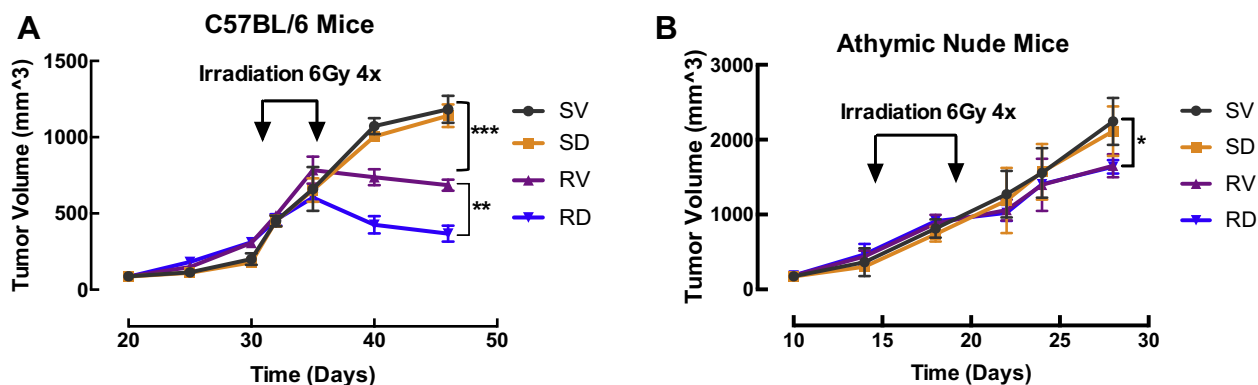


**Figure 1** Differing effects of DIM on grafted tumors after RT in immune-competent and immune-deficient mice. (A) E0771 syngeneic mammary cancer cells engrafted in C57BL/6 mice ( $n = 8$ ). Statistics using 2-way analysis of variance showed  $P < .01$  between RV and RD. (B), (C), (D) No significant difference seen in tumor volume in immune-deficient mice between RV and RD. (B) E0771 cells engrafted in Athymic nude mice ( $n = 6$ ). *Abbreviations:* DIM = 3,3'-diindolylmethane; RD = radiation + DIM; RV = radiation + vehicle; SD = sham + DIM; SV = sham + vehicle.

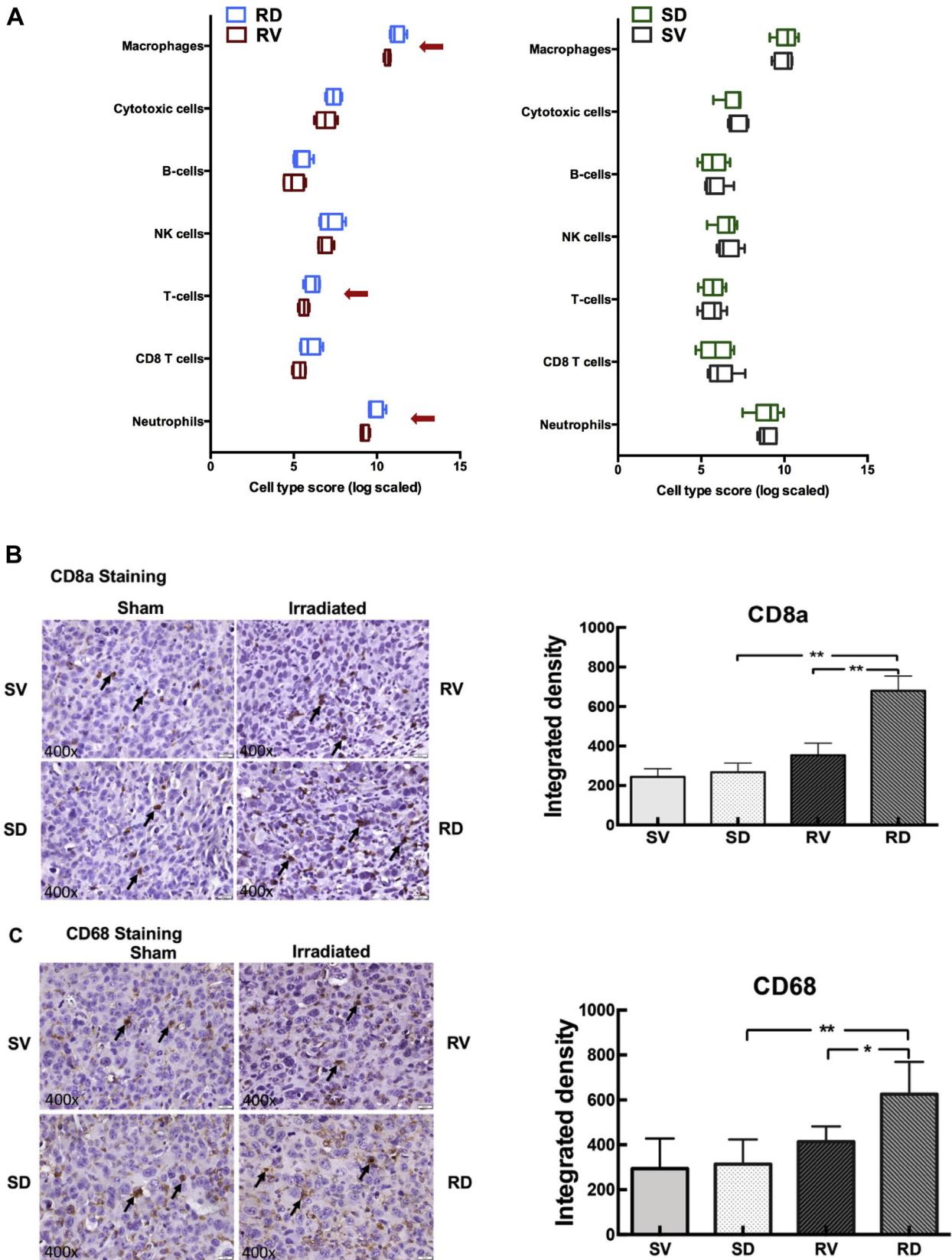


**Figure 2** Combination of 3,3'-diindolylmethane and radiation therapy increased the number of intratumoral immune cells in E0771 tumor in C57BL/6 mice. (A) Cell type profiling results of the NanoString PanCancer Immune Profiling assay. The log-scaled cell type score (x-axis) indicates the abundance of various cell types. Red arrows indicate the 3 cell types with significantly different abundances



neutrophils was significantly higher in RD compared with RV (left panel). On the other hand, without RT, abundance of these immune cells showed no significant difference regardless of DIM treatment (right panel). To visualize these 4 groups side by side, a plot combining both panels of Figure 2A is shown in Figure E4.

IHC was performed to confirm the above findings. Figure 2B and 2C shows representative images (left panels) and the integrated density of IHC staining (right panels) of tumors with CD8a<sup>+</sup> and CD68<sup>+</sup> cells, respectively. The results are consistent with the PanCancer Immune Profiling data. Both CD8a<sup>+</sup> and CD68<sup>+</sup> cells were more enriched in RD compared with RV. RV treatment showed minor increases compared with SV. DIM treatment alone (SD) had no observable effect.

### DIM combined with radiation treatment promotes immunologic responses in tumors

To reveal effects of DIM on immunologic function in tumors that received RT, the PanCancer Immune Profiling data were subjected to Pathway Scoring and Gene Set analyses. Pathway Scoring analysis condenses the gene expression profile into scores of a set of key steps in an effective antitumor immune response (Fig E5). There was little change between SV and SD groups. However, when combined with RT, DIM strongly promoted most of these immunologic processes. Plots in Figure 3A present this analysis by individual pathway. Pathways with significantly different scores between RD and RV groups, marked with red frames, cover key processes involved in antitumor immune responses. The plot comparing the pathway scores between RD and SD groups can be found in Figure E6.

Figure 3B shows the relative mRNA levels of MHC molecules and genes involved in antigen processing that were significantly higher in RD compared with RV. All 5 MHC molecules shown belong to mouse MHC class II, which is expressed exclusively in professional antigen-presenting cells. The table includes the ratio of RD versus RV, and the corresponding *P* value can be found in Table E1. To validate these results, IHC was performed using the MHC class II (I-A/I-E) antibody that specifically reacts with mouse MHC class II molecules. Consistent with the gene expression profiling data, IHC shows that RD treatment significantly increased the level of MHC class II-positive staining (Fig 3C). In addition to MHC class II genes, expression of CD74 mRNA, a chaperone and transport cofactor that assists MHC II

molecules folding and presenting,<sup>15</sup> also significantly increased using RD treatment.

### DIM combined with RT increased immune cell adhesion

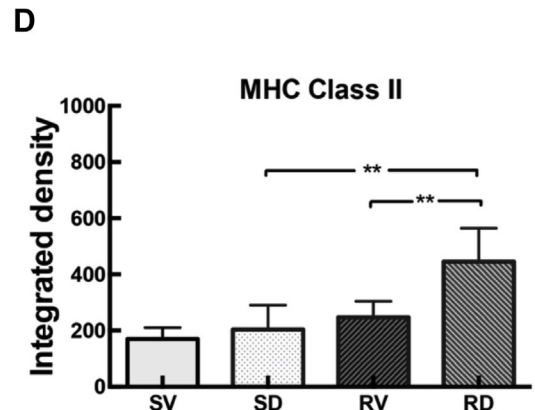
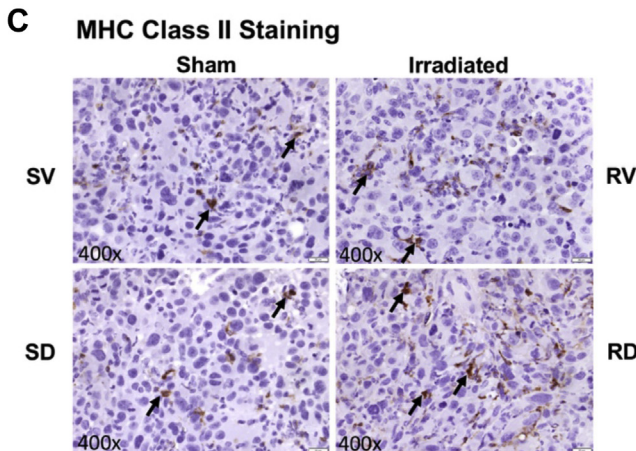
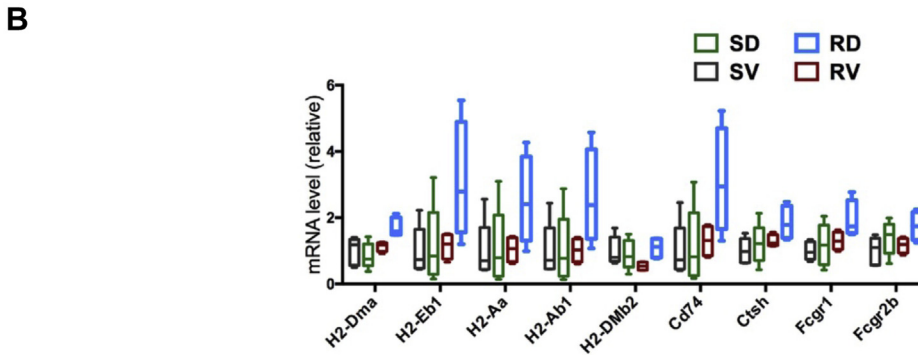
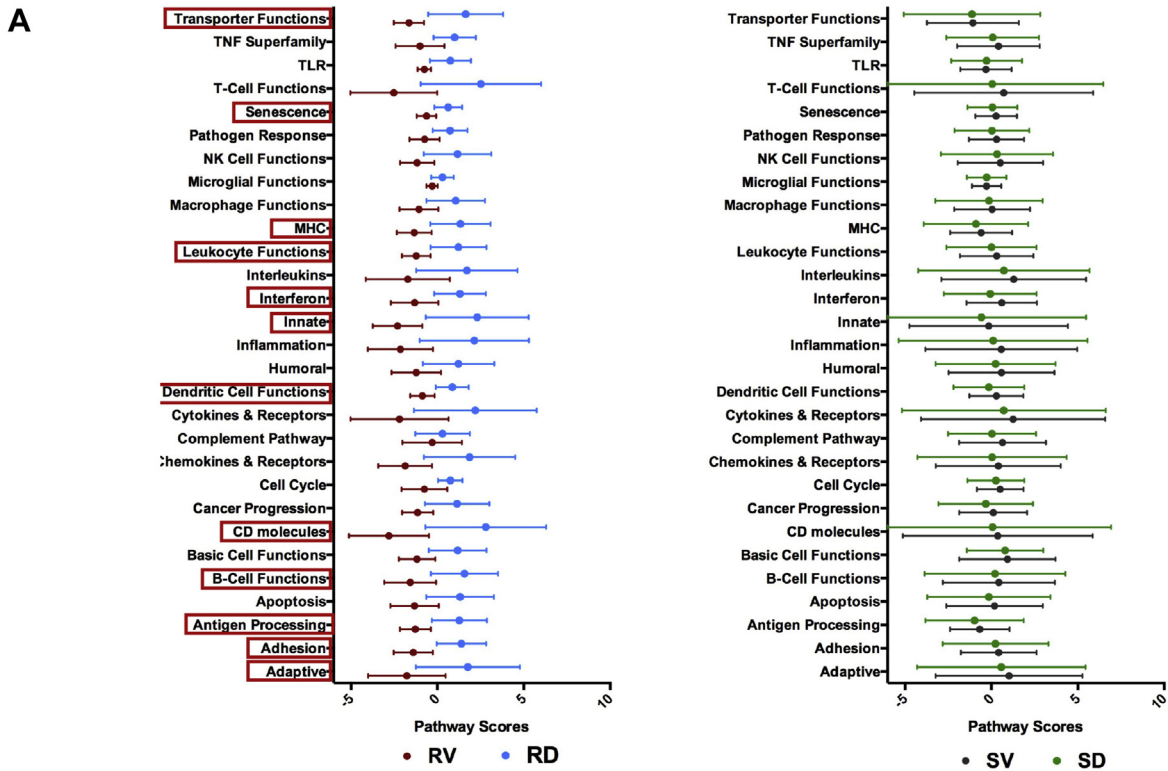
Elevated amounts of intratumoral immune cells and immune activities, such as antigen presentation, suggest increased immune cell trafficking to tumors when DIM is combined with RT. To assess angiogenesis, the pan-endothelial marker CD31 was used to detect vascular density in tumor tissues (Fig 4A and 4B). The data show a significant reduction of CD31-immunoreactive cells after radiation. DIM combined with RT reversed this reduction slightly but with no statistical significance.

Figure 4C shows the relative expression levels of genes that are implicated in the processes of cell adhesion and migration in tumor tissues. These genes showed significantly higher expression in RD compared with RV. Three of the 4 integrin genes, *Itga4*, *Itgal*, and *Itgax*, which encode integrin  $\alpha4$ ,  $\alphaL$ , and  $\alphaX$ , respectively, are expressed primarily in leukocytes. The exception, *Itga1*, is expressed in not only immune cells but also in vascular and fibroblast cells, as well as in cancer cells.<sup>16</sup> Interestingly, expression of *Vcam1*, which encodes the protein ligand for integrin  $\alpha4\beta1$  on activated endothelial cells to mediate the leukocyte-endothelial cell adhesion, also increased significantly in the presence of DIM after RT. The table includes the ratio of RD versus RV of these adhesion genes, and the corresponding *P* value can be found in Table E2. These results indicate that DIM combined with RT increased levels of adhesion molecules in immune cells and endothelial cells, which likely contributed to more immune cells enriched in irradiated tumor tissues.

### DIM combined with radiation treatment protects normal cells against the adverse effects of radiation

To address the question of how DIM augments immune cell infiltration and promotes immune activity in irradiated tumor tissues, we first explored whether DIM affects the number of leukocytes in peripheral blood. Blood samples were taken from mice that received TBI of 3 Gy or 6 Gy and were subjected to a complete blood count at 1 week postirradiation. Mice that received 3 Gy radiation combined with DIM treatment had a significantly higher relative abundance of white blood cells, red blood cells, and lymphocytes compared with mice that

(*P* < .1). Immunohistochemical staining of (B) CD8<sup>+</sup> cells and (C) CD68<sup>+</sup> cells in tumor tissues (n = 8). Representative immunohistochemistry images are shown in the left panels. The right panels show the integrated density in each treatment group. Statistics using 1-way analysis of variance are denoted by asterisks. \**P* < .05. \*\**P* < .01. (A color version of this figure is available at <https://doi.org/10.1016/j.adro.2020.10.014>.)



**Figure 3** Combination of 3,3'-diindolylmethane and radiation therapy increased levels of MHC class II molecules and enhanced antigen presentation in E0771 tumor in C57BL/6 mice. (A) Pathway score analysis of the NanoString PanCancer Immune Profiling assay. Higher score can indicate higher pathway activity. Red frames indicate pathways that showed significantly different levels

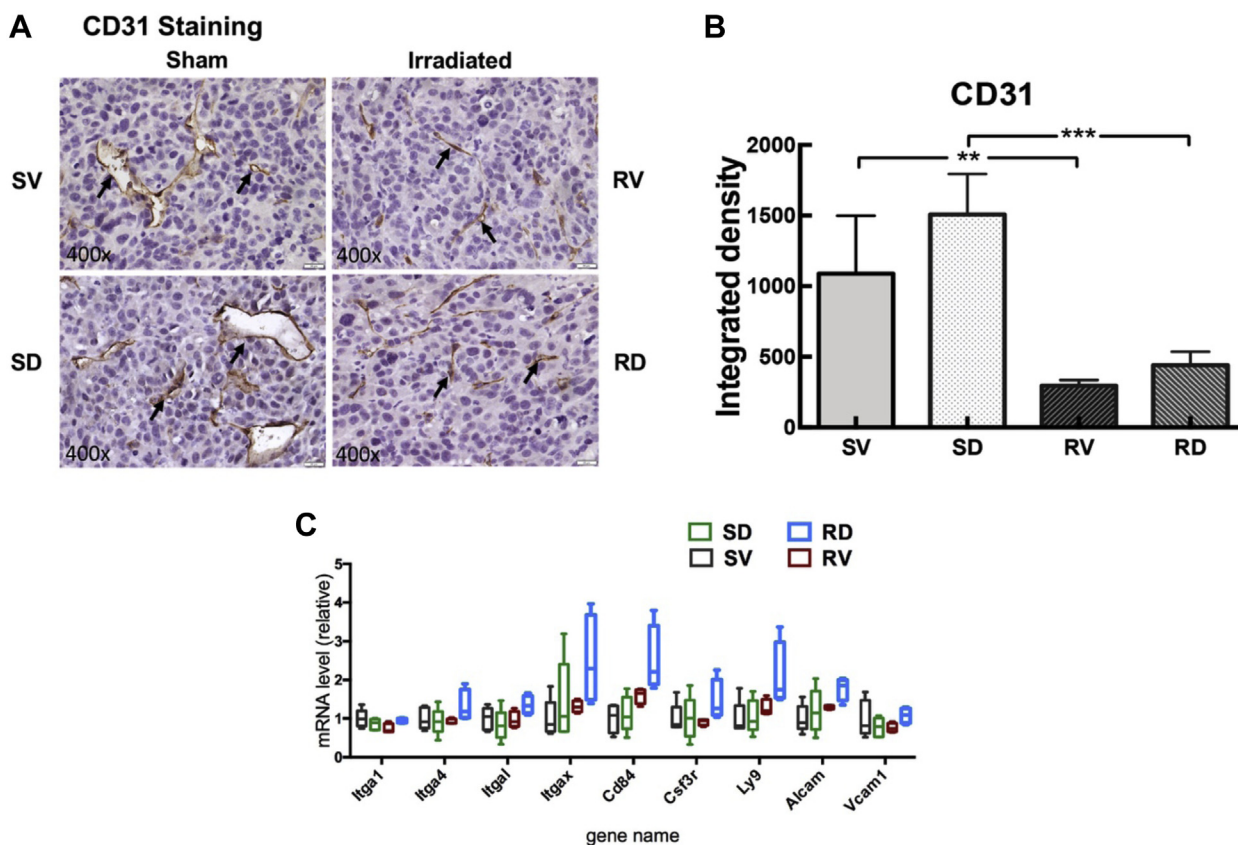


**Figure 4** Combination of 3,3'-diindolylmethane and RT significantly increased expression of adhesion genes in in E0771 tumor in C57BL/6 mice. (A) Representative immunostaining of CD31<sup>+</sup>, an endothelial marker. (B) The average integrated density of CD31<sup>+</sup> staining. Data were analyzed by 1-way analysis of variance. Asterisks denote level of statistical significance. (C) Expression level of selective genes involved in cell adhesion that were significantly different between RV and RD ( $P < .05$ ). Abbreviations: RD = radiation + DIM; RV = radiation + vehicle. \*\*  $P < .01$ . \*\*\*  $P < .001$ .

received RV treatment (Fig 5A). A similar trend was observed in mice that received 6 Gy radiation, but without statistical significance.

To investigate DIM's radioprotective effects on other normal cells, hTERT-immortalized human normal mammary epithelial cells were pretreated with either the vehicle control or 50 nM and 300 nM of DIM, followed by a dose of 3 Gy irradiation. The human breast cancer cell line MDA-MD-231 was tested in the same condition. The colony formation assay indicated that DIM treatment protected normal cells but not cancerous cells from radiation-induced cytotoxicity at both concentrations Fig 5B).

Microarray analysis was performed to examine DIM's effects on transcriptomics. The heatmap (Fig 5C) visualizes data from 1885 genes whose expression significantly changed when treated with DIM or radiation. Pathway

analysis of these genes shows enriched cell cycle, TP53 network, DNA damage response, and oxidative stress pathways (Table 1). Some of the inductions triggered by DIM treatment alone were similar to those triggered by radiation alone, although the degree of induction was weaker. These gene subsets are highlighted with yellow frames in Fig 5C. Interestingly, these genes were not induced after radiation when cells were pretreated with DIM, suggesting that DIM treatment conditioned cells so that the typical gene induction triggered by radiation was compromised.

Figure E7 shows how DIM pretreatment affects radiation-induced DNA damage signaling. As expected, radiation increased phosphorylation of BRCA1 at Ser1524, p53 at Ser15, and H2AX at Ser139. DIM pretreatment reduced these phosphorylations, indicating that

( $P < .05$ ). (B) Expression levels of selective genes in antigen presentation that were significantly different between RV and RD ( $P < .05$ ). (C) Representative immune staining of MHC class II molecules. D. The integrated density of MHC class II<sup>+</sup> in each treatment group. Statistics using 1-way analysis of variance are denoted by asterisks. Abbreviations: MHC = major histocompatibility complex; RD = radiation + DIM; RV = radiation + vehicle. \*\*  $P < 0.01$ . (A color version of this figure is available at <https://doi.org/10.1016/j.adro.2020.10.014>.)

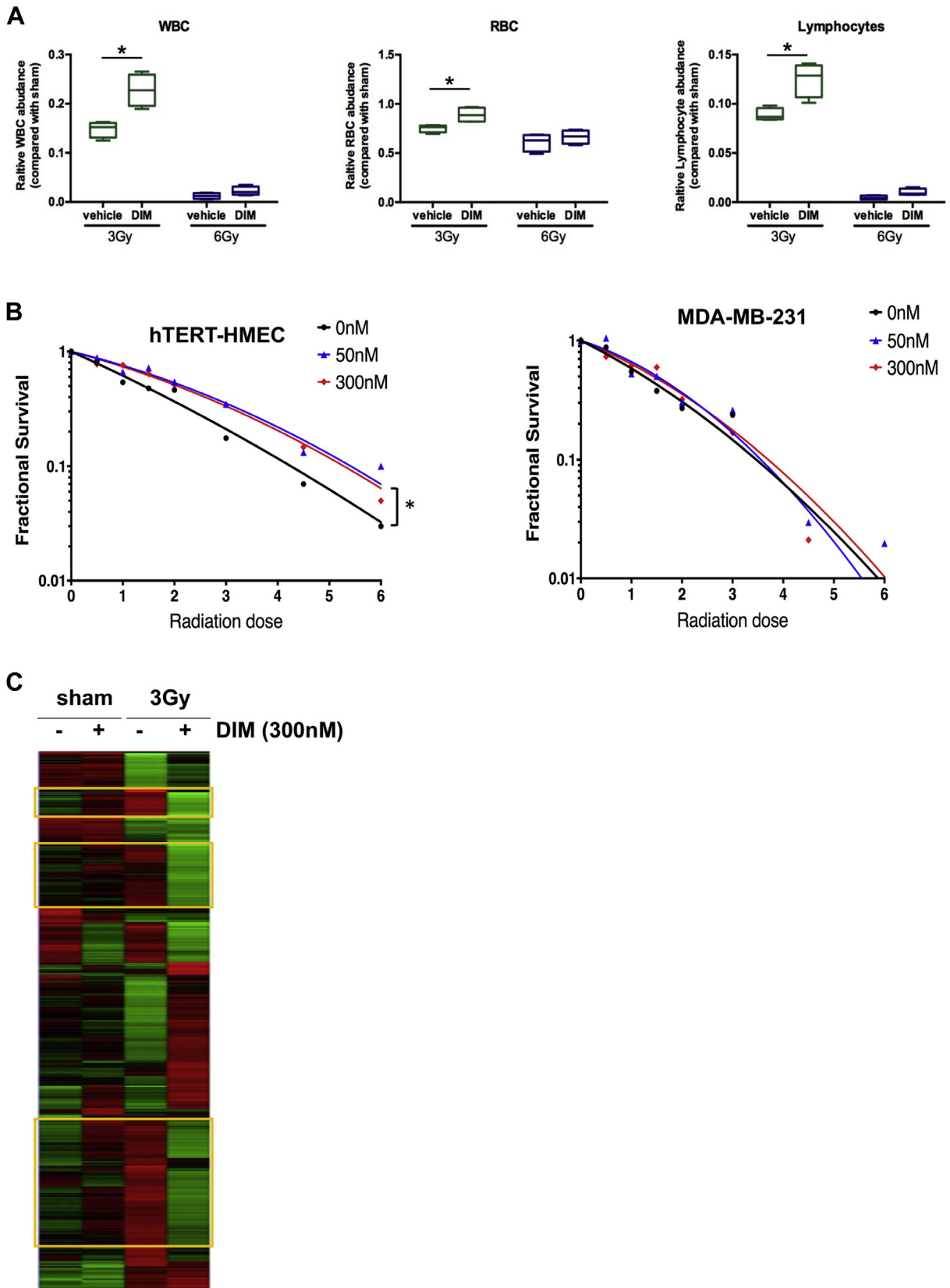


**Figure 5** DIM treatment protects normal cells against the adverse effects of radiation. (A) The relative cell abundance of circulating white blood cells, red blood cells, and lymphocytes at 1 week post-TBI (n = 6). The relative cell abundance was calculated using the average cell number of the unirradiated mice as the baseline value. (B) Clonogenic cell survival assay of hTERT-HMEC and MDA-MB-231 cells after exposure to radiation of a series of doses. DIM pretreatment at both concentrations showed a significant effect on



**Table 1** Ingenuity Pathway Analysis for 1885 genes whose expression significantly changed in hTERT-HMEC cells in any of these comparisons: 300 nM DIM treatment versus vehicle control, ionizing radiation of 3 Gy versus sham control in the absence or the presence of DIM pretreatment. *P* value indicates the significance of enrichment of specified pathway.

Pathway	<i>P</i> value	Matched entities
EGF-EGFR signaling pathway	4.15E-06	27
Cell cycle	5.56E-06	18
IL-3 signaling pathway	4.41E-05	12
Matrix metalloproteinases	7.19E-05	9
TGF beta receptor	2.96E-04	20
Interleukin 11 signaling pathway	3.65E-04	10
Serotonin receptor and signaling	8.80E-04	6
TP53 network	.002	6
MAPK signaling pathway	.002	17
Wnt pathway	.002	15
IL-9 signaling pathway	.003	5
Kit receptor signaling pathway	.004	10
DNA damage response (only ATM-dependent)	.004	8
Homologous recombination	.007	4
IL-2	.009	9
AMP-activated protein kinase signaling	.013	4
IL-1	.016	5
Oxidative stress	.016	4
Mismatch repair	.016	3
Signaling of hepatocyte growth factor receptor	.019	6
p38 MAPK signaling pathway	.019	6
BCR	.027	15
MAPK cascade	.035	5
IL-5 signaling pathway	.040	6
TCR	.048	13

Abbreviations: BCR = B cell receptor; DIM = 3,3'-diindolylmethane; EGF/EGFR = epidermal growth factor/epidermal growth factor receptor; MAPK = mitogen-activated protein kinase; TCR = T cell receptor.

the DNA damage signaling response was attenuated, a result that is consistent with the finding that those genes showed compromised induction after radiation in cells pretreated with DIM.

## Discussion

In this study, we demonstrate that DIM, when combined with RT, enhances the TIME by increasing

intratumoral immune cells and promoting expression of genes involved in key immune responses in tumors. As a result, the efficacy of radiation treatment was enhanced for tumors engrafted in immunocompetent but not immunodeficient mice. The results indicate that DIM treatment alone does not affect tumor growth, regardless of the immune conditions, suggesting that DIM's radioprotective effect on normal cells plays a critical role in promoting a TIME that favors antitumor immunity.

DIM has been shown to attenuate radiation-induced injury by inhibiting oxidative stress and cell apoptosis.<sup>5</sup> In this study, DIM treatment was found to precondition normal cells to become substantially less responsive to radiation-induced gene expression modulation. On the other hand, DIM treatment did not show radioprotection of tumor cells as, in these cells, canonical DNA damage response pathways are often malfunctioning and/or the disordered activation of survival pathways and constitutive proliferation signaling override DNA-damage-induced cell cycle arrest and apoptosis.

Lymphocytes are one of the most sensitive cell types to radiation-induced cell death. In this study, lymphocyte levels in the peripheral blood of mice that received 3 Gy TBI dropped to less than 10% of corresponding levels in the sham control 1 week after radiation. The relative lymphocyte abundance increased around 50% in mice that received TBI and DIM treatment compared with radiation with the vehicle control, a finding that is consistent with previous work.<sup>5,17</sup>

In addition to alleviating the cytotoxicity of circulating lymphocytes, protection of locoregional normal cells may also contribute to a better TIME. Radiation is known to induce apoptosis of endothelial cells through persistent p53 signaling and ceramide-mediated pathway activation.<sup>18,19</sup> In our study, vascular density was found to be reduced in irradiated tumors. Although there was no statistically significant difference, vascular density was slightly higher in mice that received RD treatment compared with RV treatment (Fig 4A, 4B), suggesting less endothelial injury. Endothelial activation can result in upregulation of adhesion molecules such as Vcam1 and cytokines, which attract immune cells to the site. Although the role of endothelial cells in tumor responses to radiation therapy remains controversial,<sup>20</sup> it is possible that radioprotection of endothelial cells and other normal cells facilitates the recruitment and infiltration of immune cells in irradiated tumors.

Our results show enrichment of T cells, neutrophils, and macrophages in irradiated tumors after RD treatment. Previous studies strongly suggest that a higher density of

radiation-induced cytotoxicity in hTERT-HMEC cells compared with the vehicle control ( $P < .05$ ). (C) Two-dimensional clustering heatmap of differential genes in conditions of 3 Gy irradiation in the absence or presence of 300 nM DIM pretreatment in hTERT-HMEC cells. Yellow frames mark subsets of genes showing common change patterns in response to RD treatment. Abbreviations: DIM = 3,3'-diindolylmethane; RD = radiation + DIM. (A color version of this figure is available at <https://doi.org/10.1016/j.adro.2020.10.014>.)

tumor-infiltrating lymphocytes (TILs) is a favorable prognostic marker for a heightened response to radiochemotherapy and better survival rates.<sup>21–23</sup> In some patients, radiochemotherapy turns “cold” tumors, which contain few TILs, to “hot” ones, with rich infiltration of T cells. Patients with tumors that remain or become “hot” after treatment show lower risk of relapse.<sup>21</sup> In the tumor model used in this study, RT alone did not significantly increase the density of infiltrated T cells, suggesting that RT by itself was not capable of effectively converting the “cold” TIME. In the presence of DIM, however, TIL density was significantly elevated after radiation (Fig 2B), and tumor regression was significantly improved (Fig 1A).

At this point, the roles of tumor-associated neutrophils (TANs) and macrophages (TAMs) remain controversial. Both pro- and antitumor roles have been reported for TANs. For example, TANs have been suggested to play a role in supporting tumor vascularization by promoting highly angiogenic MMP-9.<sup>24</sup> On the other hand, increased levels of TANs have been shown to promote higher levels of proinflammatory cytokines that are cytotoxic to tumor cells.<sup>25</sup>

Similarly, although M1-like TAMs generally exhibit antitumor activity, high infiltration of TAMs has been associated with poor clinical prognosis in patients with breast cancer.<sup>26–28</sup> In this study, IHC staining with CD68, a pan-macrophage marker, indicated that RD treatment increased TAMs but not SD treatment (Fig 2C), suggesting that these macrophages were recruited in tumors after radiation. It has been shown that the TIME usually tends to skew recruited monocytes toward the M2-like phenotype.<sup>29</sup> Our previous work demonstrated that differentiation of helper T cells to Th1 is impaired after radiation, leading to imbalanced Th1/Th2 function.<sup>30</sup> This imbalance may also contribute to macrophage polarization toward the M2-like phenotype. Considering the potential adverse effects of TAMs on the TIME, concomitant pharmacologic depletion of TAMs such as CSF1R signaling blockade<sup>31,32</sup> may boost DIM's effects in TIME modulation.

Radiation therapy is an effective treatment for cancer. Radiation eliminates cancer cells mostly by direct cytotoxicity. Preclinical and clinical data have suggested that RT acts as an immune modifier,<sup>33</sup> having both immunostimulatory and immunosuppressive effects. Radiation causes immunogenic cell death and releases autologous neoantigens to the immune system.<sup>34,35</sup> It also generates danger signals that activate stimulator of interferon genes-mediated<sup>36</sup> or Toll-like receptor<sup>37,38</sup> pathways. Given many lines of evidence supporting the notion that radiation may enrich tumor-specific effector lymphocytes and elicit priming of systemic antitumor T cell responses, it is expected that radiation treatment can be used to enhance both local and systemic antitumor immunity. It is of interest to note that abscopal effects did emerge more frequently in patients who received radiation combined

with immunotherapy.<sup>39</sup> However, these effects are often unpredictable and not seen in most patients. These puzzling findings are likely the consequence of the complex immunosuppressive effects of radiation on the TIME.

## Conclusions

In this study, using both cultured cells and preclinical breast cancer models, we show that DIM protects normal cells from cytotoxicity resulting from radiation-induced immediate DNA damage and that the combination treatment of DIM and radiation potentiates antitumor immune responses and enhances the efficacy of radiation treatment in immunocompetent mice. Our hypothesis is that the radioprotective effects of DIM on immune cells and other normal cells in the irradiated area may correct the immunosuppressive microenvironment caused by radiation. This supports the goal of developing DIM as a clinical radioprotector in cancer treatment not only by improving the therapeutic index through reducing late dose-limiting normal tissue toxicity from radiation but also by enhancing antitumor immunity.

## Supplementary Materials

Supplementary material for this article can be found at <https://doi.org/10.1016/j.adro.2020.10.014>.

## References

1. Thomson CA, Ho E, Strom MB. Chemopreventive properties of 3,3'-diindolylmethane in breast cancer: Evidence from experimental and human studies. *Nutr Rev*. 2016;74:432-443.
2. Acharya A, Das I, Singh S, et al. Chemopreventive properties of indole-3-carbinol, diindolylmethane and other constituents of cardamom against carcinogenesis. *Recent Pat Food Nutr Agric*. 2010;2:166-177.
3. Hajra S, Basu A, Singha Roy S, et al. Attenuation of doxorubicin-induced cardiotoxicity and genotoxicity by an indole-based natural compound 3,3'-diindolylmethane (DIM) through activation of Nrf2/ARE signaling pathways and inhibiting apoptosis. *Free Radic Res*. 2017;51:812-827.
4. Fan S, Meng Q, Xu J, et al. DIM (3,3'-diindolylmethane) confers protection against ionizing radiation by a unique mechanism. *Proc Natl Acad Sci U S A*. 2013;110:18650-18655.
5. Lu L, Dong J, Li D, et al. 3,3'-diindolylmethane mitigates total body irradiation-induced hematopoietic injury in mice. *Free Radic Biol Med*. 2016;99:463-471.
6. Demaria S, Coleman CN, Formenti SC. Radiotherapy: Changing the game in immunotherapy. *Trends Cancer*. 2016;2:286-294.
7. Formenti SC, Rudqvist NP, Golden E, et al. Radiotherapy induces responses of lung cancer to CTLA-4 blockade. *Nat Med*. 2018;24:1845-1851.
8. Reits EA, Hodge JW, Herberts CA, et al. Radiation modulates the peptide repertoire, enhances MHC class I expression, and induces successful antitumor immunotherapy. *J Exp Med*. 2006;203:1259-1271.
9. Hardee ME, Marciscano AE, Medina-Ramirez CM, et al. Resistance of glioblastoma-initiating cells to radiation mediated by the tumor

- microenvironment can be abolished by inhibiting transforming growth factor-beta. *Cancer Res.* 2012;72:4119-4129.
10. Vanpouille-Box C, Diamond JM, Pilonis KA, et al. TGFbeta is a master regulator of radiation therapy-induced antitumor immunity. *Cancer Res.* 2015;75:2232-2242.
  11. Bos PD, Plitas G, Rudra D, et al. Transient regulatory T cell ablation deters oncogene-driven breast cancer and enhances radiotherapy. *J Exp Med.* 2013;210:2435-2466.
  12. Kozin SV, Kamoun WS, Huang Y, et al. Recruitment of myeloid but not endothelial precursor cells facilitates tumor regrowth after local irradiation. *Cancer Res.* 2010;70:5679-5685.
  13. Deng L, Liang H, Burnette B, et al. Irradiation and anti-PD-L1 treatment synergistically promote antitumor immunity in mice. *J Clin Invest.* 2014;124:687-695.
  14. Li D, Chen R, Wang YW, et al. Prior irradiation results in elevated programmed cell death protein 1 (PD-1) in T cells. *Int J Radiat Biol.* 2018;94:488-494.
  15. Lindner R. Invariant chain complexes and clusters as platforms for MIF signaling. *Cells.* 2017;6.
  16. Alday-Parejo B, Stupp R, Rüegg C. Are integrins still practicable targets for anti-cancer therapy? *Cancers (Basel).* 2019;11.
  17. Thekkekkara D, Basavan D, Chandna S, et al. A combination of resveratrol and 3,3'-diindolylmethane, a potent radioprotector. *Int J Radiat Biol.* 2018;94:558-568.
  18. Rashi-Elkeles S, Elkon R, Shavit S, et al. Transcriptional modulation induced by ionizing radiation: p53 remains a central player. *Mol Oncol.* 2011;5:336-348.
  19. Kolesnick R, Fuks Z. Radiation and ceramide-induced apoptosis. *Oncogene.* 2003;22:5897-5906.
  20. Guipaud O, Jaillet C, Clément-Colmou K, et al. The importance of the vascular endothelial barrier in the immune-inflammatory response induced by radiotherapy. *Br J Radiol.* 2018;91, 20170762.
  21. Dieci MV, Mathieu MC, Guarneri V, et al. Prognostic and predictive value of tumor-infiltrating lymphocytes in two phase III randomized adjuvant breast cancer trials. *Ann Oncol.* 2015;26:1698-1704.
  22. Pagès F, Galon J, Dieu-Nosjean MC, et al. Immune infiltration in human tumors: A prognostic factor that should not be ignored. *Oncogene.* 2010;29:1093-1102.
  23. Bayraktar S, Batoo S, Okuno S, et al. Immunotherapy in breast cancer. *J Carcinog.* 2019;18:2.
  24. Deryugina EI, Zajac E, Juncker-Jensen A, et al. Tissue-infiltrating neutrophils constitute the major in vivo source of angiogenesis-inducing MMP-9 in the tumor microenvironment. *Neoplasia.* 2014;16:771-788.
  25. Fridlender ZG, Sun J, Kim S, et al. Polarization of tumor-associated neutrophil phenotype by TGF-beta: "N1" versus "N2" TAN. *Cancer Cell.* 2009;16:183-194.
  26. Tang X. Tumor-associated macrophages as potential diagnostic and prognostic biomarkers in breast cancer. *Cancer Lett.* 2013;332:3-10.
  27. Poh AR, Ernst M. Targeting macrophages in cancer: from bench to bedside. *Front Oncol.* 2018;8:49.
  28. Qiu SQ, Waaijer SJH, Zwager MC, et al. Tumor-associated macrophages in breast cancer: Innocent bystander or important player. *Cancer Treat Rev.* 2018;70:178-189.
  29. Xu M, Liu M, Du X, et al. Intratumoral delivery of IL-21 overcomes anti-Her2/Neu resistance through shifting tumor-associated macrophages from M2 to M1 phenotype. *J Immunol.* 2015;194:4997-5006.
  30. Chen R, Wang YW, Fornace AJ, et al. Impairment of the intrinsic capability of Th1 polarization in irradiated mice: A close look at the imbalanced Th1/Th2 response after irradiation. *Radiat Res.* 2016; 186:559-567.
  31. Ries CH, Cannarile MA, Hoves S, et al. Targeting tumor-associated macrophages with anti-CSF-1R antibody reveals a strategy for cancer therapy. *Cancer Cell.* 2014;25:846-859.
  32. Dammeijer F, Lievens LA, Kaijen-Lambers ME, et al. Depletion of tumor-associated macrophages with a CSF-1R kinase inhibitor enhances antitumor immunity and survival induced by DC immunotherapy. *Cancer Immunol Res.* 2017;5:535-546.
  33. Demaria S, Golden EB, Formenti SC. Role of local radiation therapy in cancer immunotherapy. *JAMA Oncol.* 2015;1:1325-1332.
  34. Nessel JP, Schae D, McBride WH, et al. Irradiation to improve the response to immunotherapeutic agents in glioblastomas. *Adv Radiat Oncol.* 2019;4:268-282.
  35. Wennerberg E, Vanpouille-Box C, Bornstein S, et al. Immune recognition of irradiated cancer cells. *Immunol Rev.* 2017;280:220-230.
  36. Deng L, Liang H, Xu M, et al. STING-dependent cytosolic DNA sensing promotes radiation-induced type I interferon-dependent antitumor immunity in immunogenic tumors. *Immunity.* 2014;41:843-852.
  37. Haikerwal SJ, Hagekyriakou J, MacManus M, et al. Building immunity to cancer with radiation therapy. *Cancer Lett.* 2015;368:198-208.
  38. Wang HT, Lee HI, Guo JH, et al. Calreticulin promotes tumor lymphocyte infiltration and enhances the antitumor effects of immunotherapy by up-regulating the endothelial expression of adhesion molecules. *Int J Cancer.* 2012;130:2892-2902.
  39. Golden EB, Chhabra A, Chachoua A, et al. Local radiotherapy and granulocyte-macrophage colony-stimulating factor to generate abscopal responses in patients with metastatic solid tumors: A proof-of-principle trial. *Lancet Oncol.* 2015;16:795-803.